Supporting Information

Hoboth et al. 10.1073/pnas.1409542112

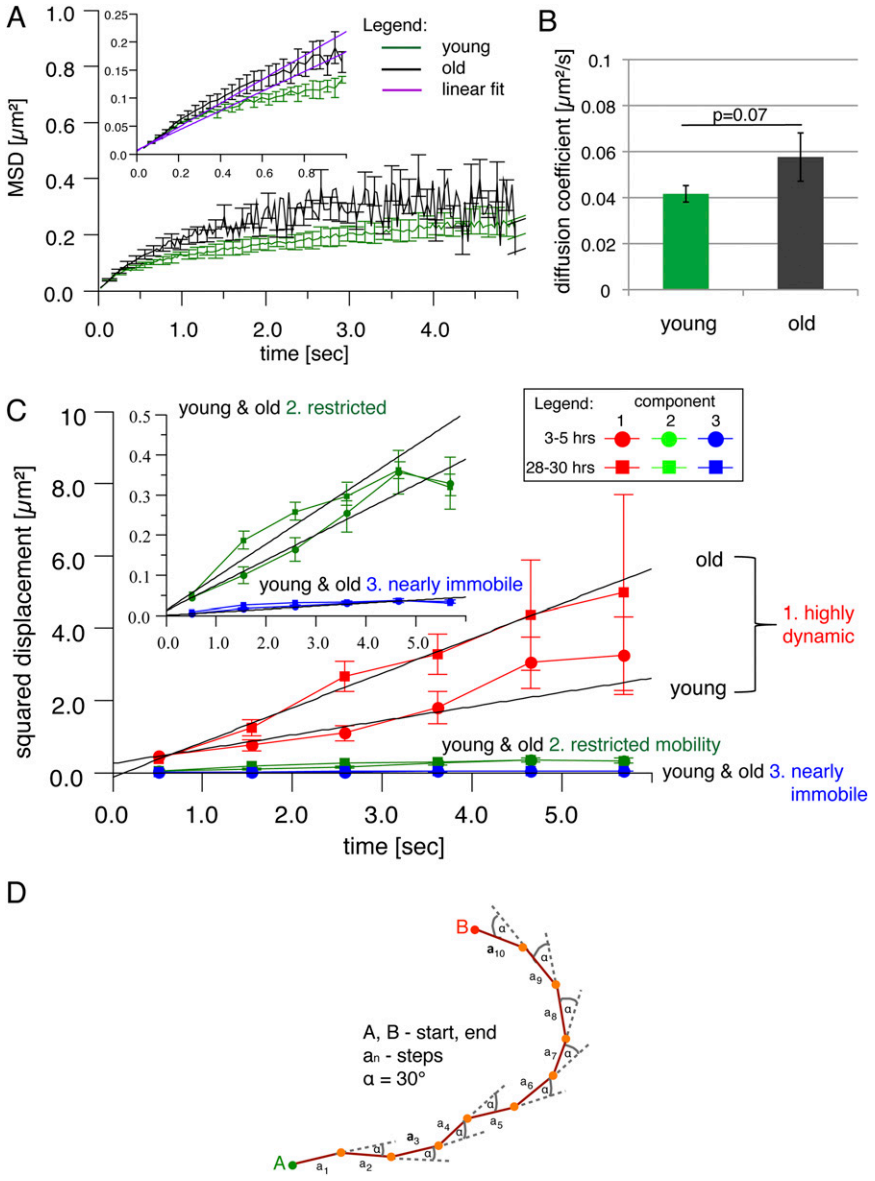

Fig. S1. Analysis of the dynamic components. (*A*) Mean squared displacement (MSD) as a function of time for 3- to 5- and 28- to 30-h-old Ins-SNAP$^{TMR\text{-}Star+}$ SGs. (*Inset*) MSD per time in the smaller time interval of the first 1 s. (*B*) The diffusion coefficients were calculated according to the equation MSD = 4DΔt based on the linear fit (*A*, *Inset*) obtained by regression analysis. (*C*) Squared displacement as a function of time for each of the dynamic components contributing to the collective motion of young and old SGs and the corresponding linear fit (black line) used to calculate diffusion coefficients. (*Inset*) Squared displacement as a function of time for restricted and nearly immobile components at higher resolution. (*D*) Schematic representation of processive movements defined as a minimum of 10 steps between A and B without changes in direction >30° in between each step.

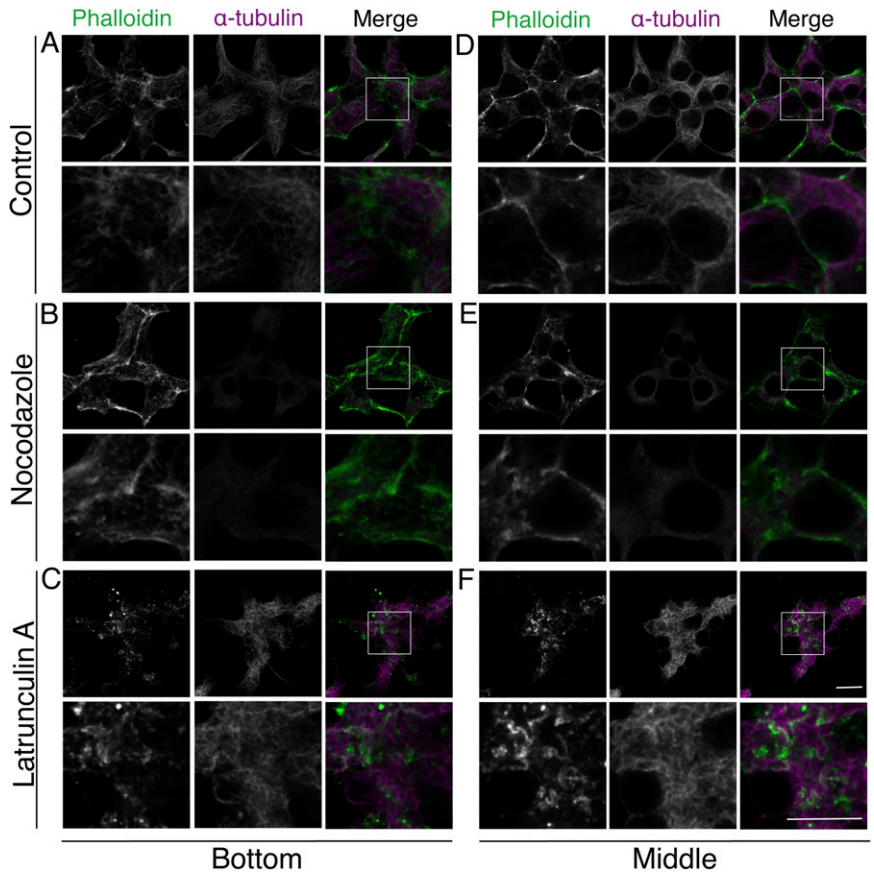

Fig. S2. Effects of nocodazole or latrunculin A treatment on MTs and FA. (*A*–*F*) Confocal images of INS-1 cells untreated (*A* and *D*) or treated with 16.6 μM nocodazole for 60 min (*B* and *E*) or 1 μM latrunculin A for 30 min (*C* and *F*) and then labeled for α-tubulin and OG–phalloidin. *A*–*C* show optical sections of cells close to the coverslip (Bottom), and *D* and *E* show optical sections throughout the cells (Middle). The bottom row of each panel is a higher magnification of the region boxed in the corresponding top raw. (Scale bars, 10 μm.)

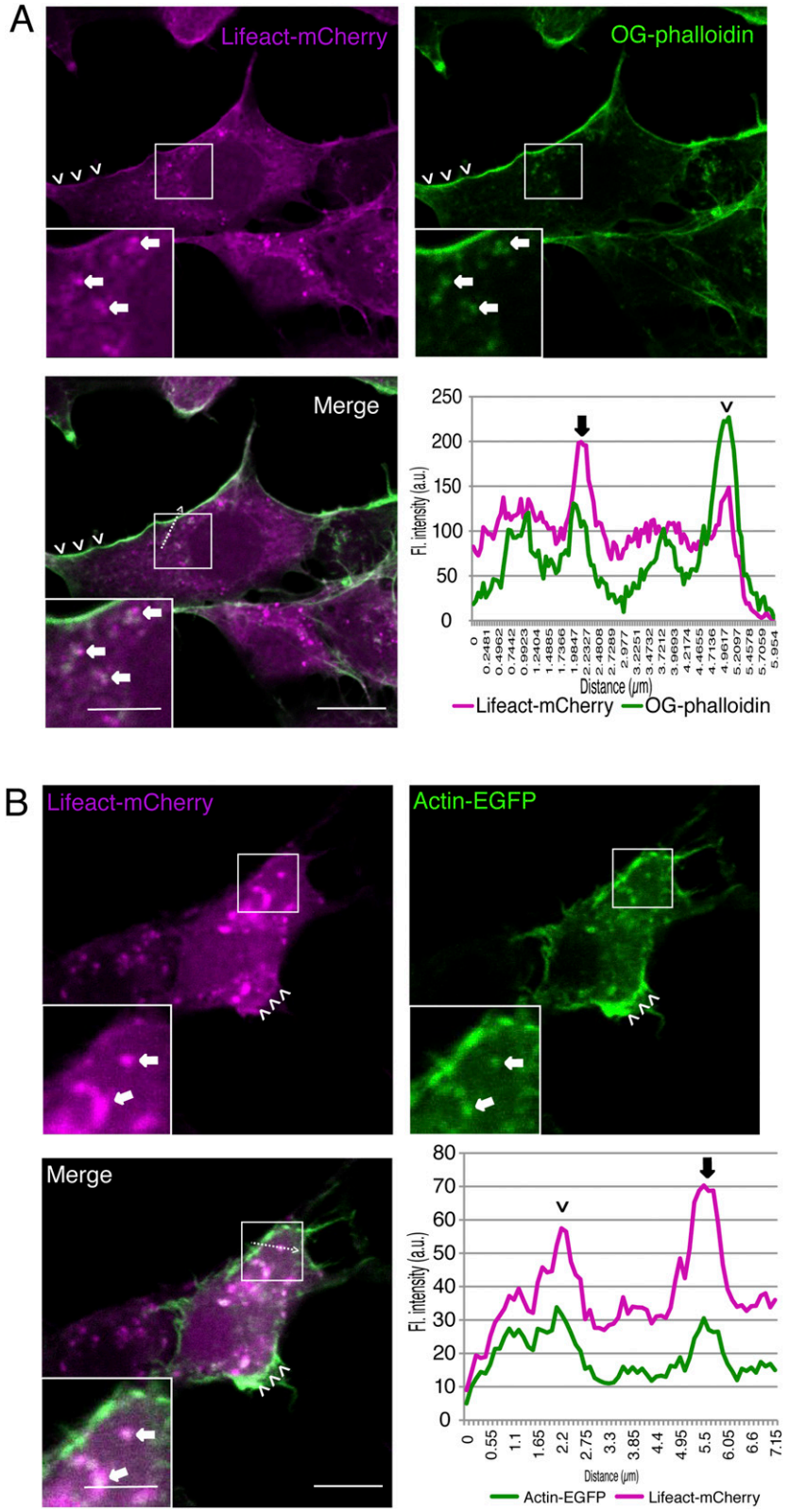

Fig. S3. Lifeact-mCherry is specific for FA. (*A*) Confocal images of INS-1 cells expressing Lifeact-mCherry and labeled with OG–phalloidin. (*Insets*) The boxed regions at higher magnification. Arrows indicate objects double-positive for Lifeact-mCherry and OG–phalloidin; arrowheads indicate the peripheral FA rim. Also shown is the fluorescence intensity profile along the dotted line crossing an object (arrow) as well as the peripheral rim (arrowhead). (Scale bars: 5 μm; inset, 1 μm.) (*B*) Confocal images of INS-1 cells expressing Lifeact-mCherry and β-actin-EGFP. (*Insets*) Higher magnifications of the boxed regions. Arrows indicate objects double-positive for Lifeact-mCherry and β-actin-EGFP; arrowheads indicate the peripheral FA rim. Also shown is the fluorescence intensity profile along the dotted line crossing an object (arrow) as well as the peripheral rim (arrowhead). (Scale bars: 5 μm; inset, 1 μm.)

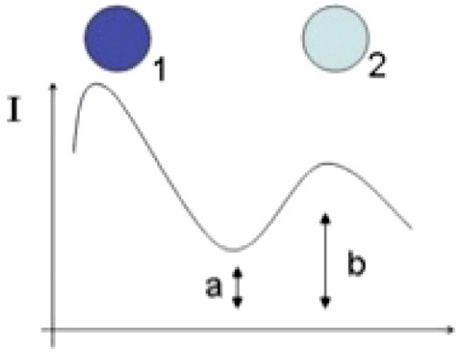

Fig. S4. Object combination coefficient. During object search, the software often finds two or more objects very close to one another. These objects may be combined into a single object for tracking. Combination depends on the object combination coefficient. The value ranges from 0 to 1, with 0 = never to combine objects and 1 = always combine objects. In our analyses we used object combination coefficient 0.95. This figure illustrates the calculation of the object combination coefficient that is given by the ratio between the intensity (I) of a and b. Two objects (1, 2) will be combined if the ratio a/b < object combination coefficient.

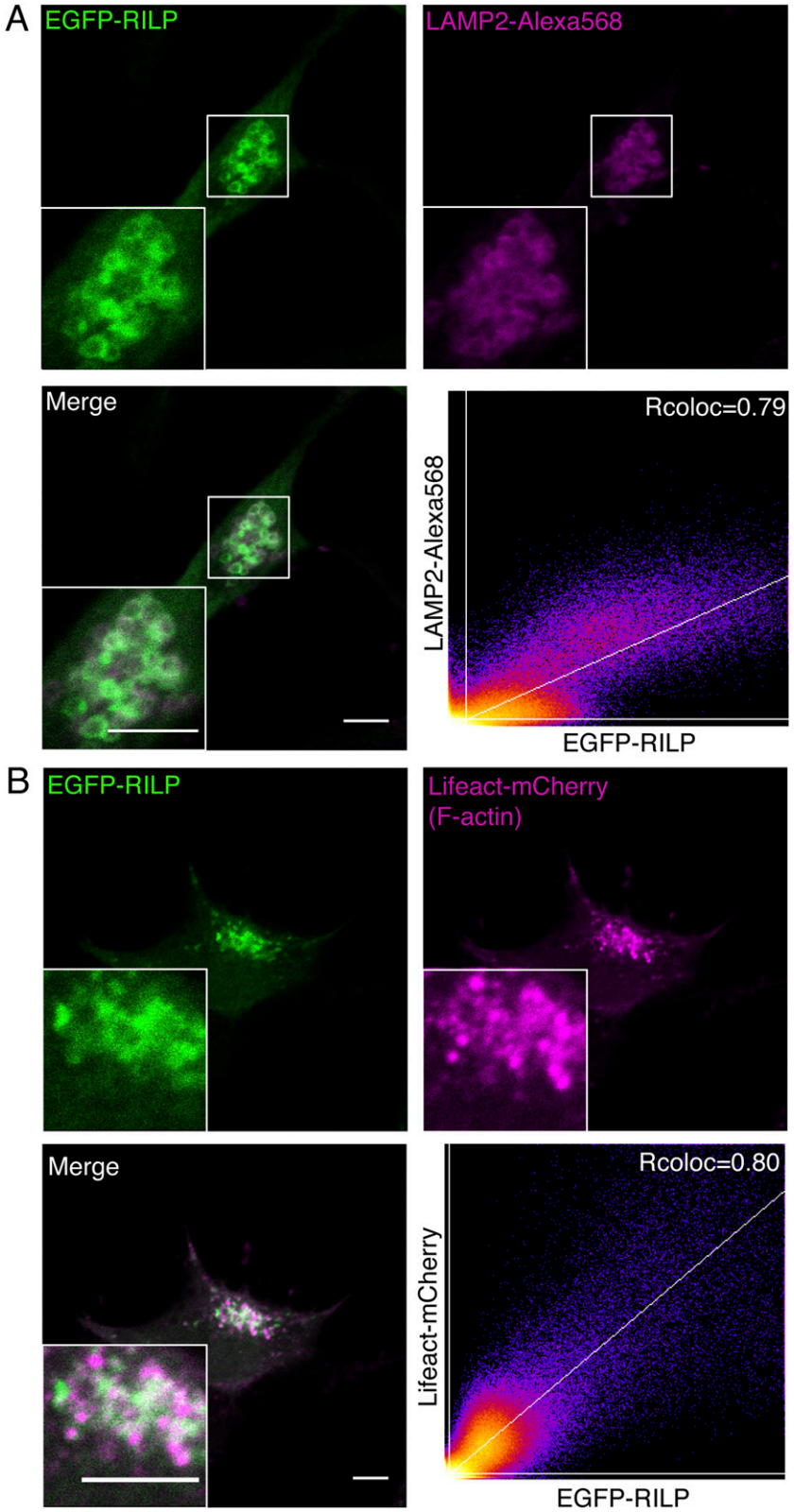

Fig. S5. EGFP-RILP colocalizes with LAMP2 and Lifeact-mCherry. (*A*) Confocal images of INS-1 cells expressing EGFP-RILP and labeled for LAMP2. (*Insets*) Higher magnification of the boxed regions. Scatter plots and Rcoloc, as calculated with the imaging software Fiji, document the colocalization of EGFP-RILP and LAMP2-Alexa568. (Scale bars, 5 μm.) (*B*) Confocal images of INS-1 cells expressing EGFP-RILP and Lifeact-mCherry. (*Insets*) Higher magnification of the boxed regions. Scatter plot and Rcoloc documents the colocalization of EGFP-RILP and Lifeact-mCherry. (Scale bars, 5 μm.)

Table S1. Log probabilities resulting from the fitting of our experimental data to the models postulating existence of two, three, and four dynamic components accounting for the collective SG dynamics

Tested scenario	Younger SG population	Older SG population
Two components	−1,602	−1,433
Three components	−1,315	−1,237
Four components	−1,464	−1,370

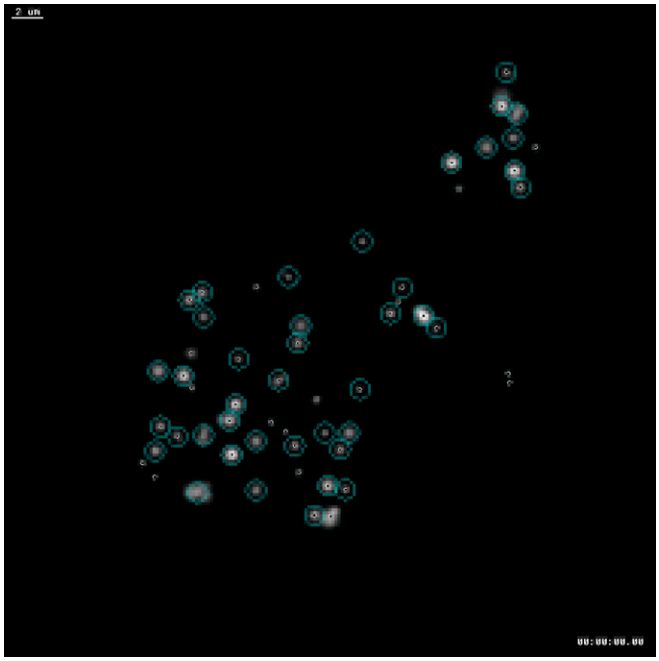

Movie S1. TIRFM and Motion Tracking analysis of Ins-SNAP$^{TMR\text{-}Star+}$ SGs. TIRFM video of young Ins-SNAP$^{TMR\text{-}Star+}$ SGs in living INS-1 cell was processed with Motion Tracking software to create a synthetic image and track Ins-SNAP$^{TMR\text{-}Star+}$ objects.

Movie S1

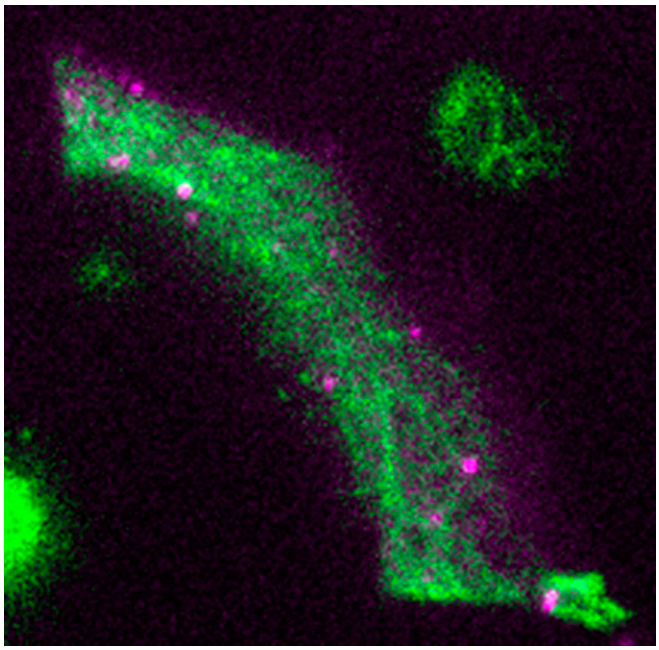

Movie S2. Ins-SNAP$^{TMR\text{-}Star+}$ SGs move on MTs. TIRFM video of young Ins-SNAP$^{TMR\text{-}Star+}$ SGs (magenta) shows their movement on MTs in living INS-1 cell expressing α-tubulin-GFP (green).

Movie S2

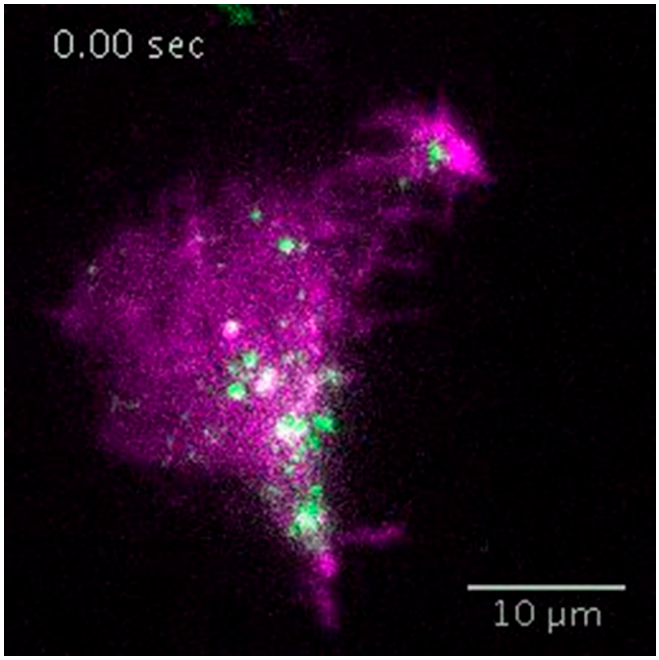

Movie S3. Old SGs are FA^{+}. TIRFM video shows overlap of some old Ins-SNAP^{OG+} SGs (green) with Lifeact-mCherry (magenta) and their movement in living INS-1 cells.

Movie S3

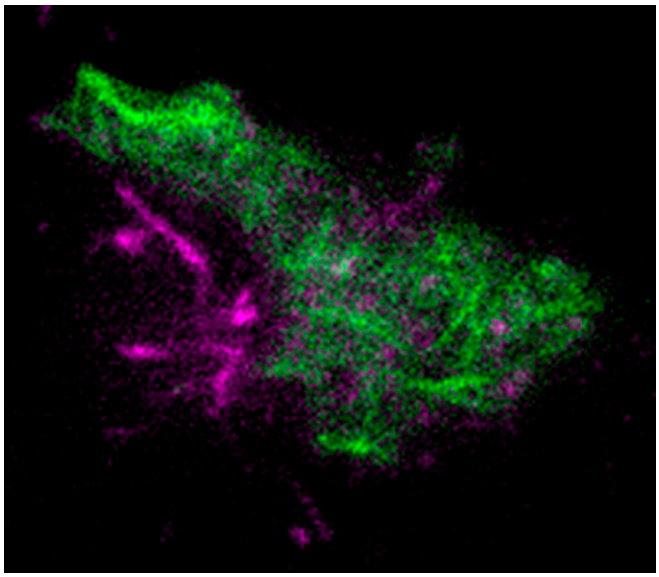

Movie S4. FA^+ vesicles move on MTs. TIRFM video documents movement of Lifeact-$mCherry^+$ vesicles on MTs in living INS-1 cell expressing α-tubulin-GFP (green).

Movie S4

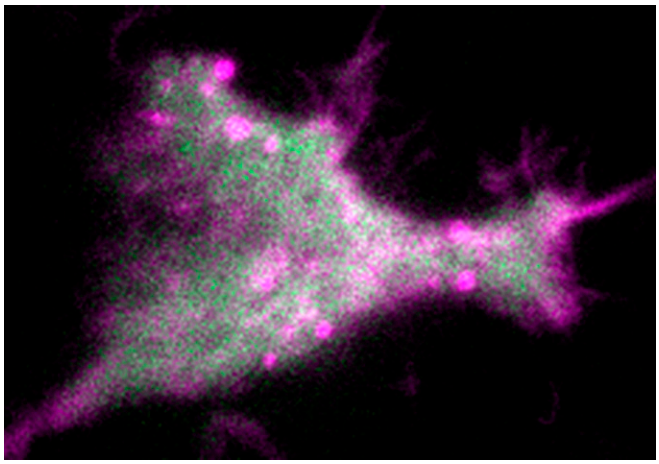

Movie S5. Motion of FA^+ vesicles is impaired by the disruption of MTs. TIRFM video illustrates impaired movement of Lifeact-$mCherry^+$ vesicles in living INS-1 cell expressing α-tubulin-GFP (green) and treated with nocodazole.

Movie S5